

Targeting homologous recombination by pharmacological inhibitors enhances the killing response of glioblastoma cells treated with alkylating drugs

Nancy Berte¹, Andrea Piée-Staffa¹, Nadine Piecha¹, Mengwan Wang¹, Kerstin Borgmann²,
Bernd Kaina^{1*}, Teodora Nikolova^{1*}

¹Institute of Toxicology, University Medical Center Mainz, Germany

²Laboratory of Radiobiology & Experimental Radiooncology, Center of Oncology, University
Medical Center Hamburg-Eppendorf, Germany

*Corresponding authors:

Institute of Toxicology
University Medical Center
Obere Zahlbacher Str. 67
D-55131 Mainz
Germany

Key Words:

Glioblastoma multiforme, homologous recombination targeting, chemotherapy

Running title:

Targeting homologous recombination in glioma chemotherapy

Conflict of interest:

Authors declare there is no conflict of interest.

Financial information:

This work was supported by DFG (German Research Foundation), grant Ni1319/1–1 and Ni1319/1-2 and by a grant from the Internal Research Funding of University Mainz to T.N. (2015-2016).

Abstract

Malignant gliomas exhibit a high level of intrinsic and acquired drug resistance and have a dismal prognosis. First and second line therapeutics for glioblastomas are alkylating agents, including the chloroethylating nitrosoureas (CNU) lomustine, nimustine, fotemustine and carmustine. These agents target the tumor DNA, forming O^6 -chloroethylguanine adducts and secondary DNA interstrand crosslinks (ICLs). These crosslinks are supposed to be converted into DNA double-strand breaks, which trigger cell death pathways. Here, we show that lomustine (CCNU) with moderately toxic doses induces ICLs in glioblastoma cells, inhibits DNA replication fork movement and provokes the formation of DSBs and chromosomal aberrations. Since homologous recombination (HR) is involved in the repair of DSBs formed in response to CNU, we elucidated whether pharmacological inhibitors of HR might have impact on these endpoints and enhance the killing effect. We show that the Rad51 inhibitors RI-1 and B02 greatly ameliorate DSBs, chromosomal changes and the level of apoptosis and necrosis. We also show that an inhibitor of MRE11, mirin, which blocks the formation of the MRN complex and thus the recognition of DSBs, has a sensitizing effect on these endpoints as well. In a glioma xenograft model, the Rad51 inhibitor RI-1 clearly enhanced the effect of CCNU on tumor growth. The data suggests that pharmacological inhibition of HR, e.g. by RI-1, is a reasonable strategy for enhancing the anticancer effect of CNU.

Introduction

Glioblastoma multiforme (GBM) is the most prevalent type of primary malignant brain tumor in adults, which is known for its aggressive progression, weak response to cancer therapy and, consequently, bad prognosis [1, 2]. The poor overall 5-year survival of less than 10% points to the need of new chemotherapeutic approaches. The today's standard care of GBM includes maximal surgical resection followed by radiation and concomitant temozolomide treatment followed by adjuvant temozolomide cycles [1-3]. Chloroethylating nitrosoureas (CNU), including lomustine (CCNU), nimustine (ACNU), semustine (MeCCNU), carmustine (BCNU) and fotemustine have been used as second-line drugs for the treatment of GBM. Lomustine can be administered orally [4] and, therefore, it is currently preferentially in use. CNU can also be applied for first-line therapy in the form of BCNU wafers (Gliadel®) installed into the operative wound, the so-called localized chemotherapy for high-grade glioma [1]. CNU are also applied for second-line chemotherapy of metastatic melanoma, Hodgkin lymphoma and brain metastases of different origin [5-10].

The mechanism of alkylating agents including CNU has been intensively studied [11]. They chloroethylate DNA and induce a broad spectrum of DNA adducts with O⁶-chloroethylguanine being the main killing lesion. This adduct is unstable and undergoes intramolecular rearrangement leading to an intermediate, N1-O⁶-ethenoguanine, and finally to N1-guanine-N3-cytosine interstrand cross-link (ICLs) [12]. The critical primary lesion, O⁶-chloroethylguanine, is subject to repair by transfer of the alkyl group to O⁶-methylguanine-DNA methyltransferase (MGMT) [13]. This repair process renders cancer cells resistant to chloroethylating chemotherapeutics [14-17]. The activity of MGMT in brain tumours is highly variable; 17% of pretreatment tumors do not display MGMT activity and up to 30% express MGMT at low level [18, 19]. In these tumours O⁶CIEG remains unrepaired and the cytotoxic ICLs can be formed. In tumors with positive MGMT status, repeated treatment with a methylating anticancer drug causes MGMT to be used up by the repair reaction, which can be harnessed to deplete MGMT and to enhance the tumor cell killing response. Actually, coadministration of procarbazine and CCNU improved the therapeutic index for GBM patients [20].

ICLs are lesions that block replication fork movement. They can be removed by a complex repair pathway, allowing the restart of DNA replication [21]. The repair of ICLs involves the transient formation of DNA double-strand breaks (DSBs) by endonucleases at the site of the stalled replication fork [22, 23]. Blocked replication and DSB intermediates activate the DNA damage response and downstream apoptotic pathways [24, 25]. Since DSBs formed during ICL repair are critical secondary DNA lesions, it is reasonable to posit that their repair determines tumor cell resistance to CNU. Two DSB repair pathways have been described, namely homologous recombination (HR) and non-homologous end-joining (NHEJ) [26]. NHEJ represents the major pathway for the repair of DSBs induced by ionizing radiation in G0/G1 [27]. It is considered to be error-prone, giving rise to chromosomal aberrations [28]. In contrast, HR repair of DSBs is operative in late S/G2 and involves strand invasion onto the sister chromatid template, DNA repair synthesis and resolution of the Holiday junction [29]. Usage of the undamaged template ensures error-free DSB repair. Mre11 is an endo- and exonuclease, which participates in the recognition of DSBs *via* the MRN complex together with Rad50 and NBS1 (alias NBN). It also acts as a multi-functional DNA end-processing enzyme and plays a role in the restart of stalled replication forks by enhancing the resection at stalled forks, as shown for BRCA2-deficient cells [30, 31]. The key HR protein is Rad51 because of its recombinase activity. Rad51 overexpression has been observed by immunohistochemistry in various cancers, e.g. breast, pancreas, head and neck, lung, oesophageal and colon [32-36] and also in gliomas [37], while no detectable expression was

found in normal differentiated tissues from the same organs [32-35]. In most studies Rad51 overexpression was associated with poor prognosis for the patients.

Investigating the role of HR and NHEJ in the cellular sensitivity to CNU, we showed that HR defective cells (BRCA2, Rad51D and XRCC3 mutants) are hypersensitive to ACNU whereas NHEJ defective cells (Ku80 and DNA-PK mutants) were not or only mildly sensitive to the drug [25]. This pertained the endpoints reproductive survival, apoptosis and chromosomal breakage [25]. Since HR plays a pivotal role in cellular protection against DNA alkylation-induced killing effects, it is reasonable to posit that pharmacological inhibition of HR is a way of cancer sensitization. In the present study, we tested this hypothesis in human glioblastoma cell lines by targeting HR repair proteins pharmacologically. We used the MRE11 inhibitor mirin [38] and the Rad51 inhibitors B02 [39, 40] and RI-1 [41, 42] for inhibiting the DNA damage response (DDR) and HR, respectively, following treatment of cells with CCNU. We also studied RI-1 in combination with CCNU in a glioblastoma xenograft model. The data show that pharmacological inhibition of MRE11 and HR is a feasible strategy for sensitizing glioblastoma cells to CNU.

Material and Methods

Cell lines and culture

The human glioma cell line LN229 was obtained from ATCC (USA), U87MG from CLS Cell Line Service (Eppelheim, Germany) and LN308 cells were provided by Dr. N. de Tribolet (Lausanne, Switzerland). LN229 and U87MG were authenticated by ATCC. LN308 was not further authenticated. The lines were kept frozen and used at early passage after receipt. They were previously characterized regarding their MGMT status [18, 43], karyotyped and tested monthly for mycoplasma contamination. Cells were maintained in advanced DMEM (Life Technologies, Darmstadt, Germany) supplemented with L-glutamine and 5 or, for the colony formation assay, 10% of fetal bovine serum (Gibco, Life technologies) at 37°C in a humidified atmosphere with 7% CO₂.

Treatment with CCNU and pharmacological inhibitors

ACNU (nimustine hydrochloride from Sigma-Aldrich, Taufkirchen, Germany) was diluted in sterile bi-distilled water, whereas CCNU (lomustine from Sigma-Aldrich) was diluted in absolute ethanol to give a concentration of 10 mM and added to the cell culture medium or additionally diluted in medium to give final concentrations in the range of 5–50 µM. In all assays, cells were pulse treated with CCNU for 1 h. Thereafter the medium was replaced by

fresh medium. Mirin (Tocris Bioscience, Bristol, UK), as well as B02 and RI-1 (both from Axon MedChem, Groningen, The Netherlands) were diluted in DMSO to give a concentration of 25 mM and added to cell cultures to give final concentrations of 2.5-25 μ M. Cells were further incubated until harvesting. Chemical structures of CCNU, B02, Mirin and RI-1 are shown in Suppl. Figure 1.

Modified alkaline comet assay for measurement of ICLs

Cross-link formation and repair were measured by a modified version of the alkaline comet assay (single cell electrophoresis, SCGE) as previously described [44]. Briefly, exponentially growing LN229, LN308 or U87MG cells were treated for 1 h with 50 μ M CCNU. Untreated and treated cells were harvested after 24, 48 or 72 h in PBS at a density of 2.5×10^5 cells/ml and irradiated with 8 Gy γ -rays. The radiation was generated by ^{137}Cs (1800 Ci) in a Gammacell 2000 device (Molsgaard Medical) at 7.7 rad/s [45]. It is known that fragmentation of genomic DNA by ionizing radiation leads to comet formation, while induced ICLs reduce the mobility of DNA, resp. the length and fluorescence intensity of the comets. Micro-gels were prepared by embedding single cells in low melting point agarose onto agarose-coated slides and standard alkaline SCGE was done as described [44]. Propidium iodide (PI) stained slides were evaluated using a fluorescence microscope (Nikon Instruments Europe, Düsseldorf, Germany) and the Comet IV software (Perceptive Imaging, Liverpool, UK). The results are expressed as tail intensity comparing γ -ray irradiated cells after CCNU and cells treated with γ -rays only.

Homologous recombination activity assay

To measure the capacity of cells to repair DSB by HR, LN229 cells were stably transfected with a pDRGFP plasmid (Addgene, Cambridge, USA). The plasmid bears two non-functional GFP genes. One truncated, the other containing a recognition site for I-SceI endonuclease. Upon transient transfection with I-SceI expressing plasmid (Addgene), the endonuclease cleaves the modified GFP gene leading to a DSB. If this DSB is repaired via HR, by means of the sequence of the truncated GFP gene, a functional GFP protein is generated and can be quantified by flow cytometry. Cells were analyzed 72 h after transfection with 1 μ g p β ASceI using the transfection kit Effectene (Quiagen). During transfection, the cells were incubated in the presence or absence of 10 μ M B02, 25 μ M mirin or 25 μ M RI-1. The DNA-PK inhibitor KU0060648 (Selleckchem) was used for comparison at a final concentration of 1 μ M. We expected that the inhibition of DNA-PK leads to a moderate increase in HR activity due to the lack of competition by NHEJ for the repair of DSB [46]. Cells were trypsinized and washed with PBS and measured by flow cytometry using FACS Canto II (BD Biosciences). Data were analyzed with BD FACSDiva™ software.

DNA fiber assay

The DNA fiber assay was performed as described [47]. Briefly, exponentially growing cells were treated with 30 μM CCNU and further incubated in the presence or absence of 10 μM B02, 25 μM mirin or 25 μM RI-1 for 6 or 16 h, then pulse labelled with 25 μM 5-chloro-2'-deoxyuridine (CldU, Sigma-Aldrich) followed by labelling with 250 μM 5-iodo-2'-deoxyuridine (IdU) (TCI Deutschland, Eschborn, Germany) for 30 min each. Labelled cells were harvested and DNA fiber spreads prepared. Acid treated fiber spreads were stained with monoclonal rat anti-BrdU (Oxford Biotechnologies, 1:1000) followed by monoclonal mouse anti-BrdU (Becton–Dickinson, 1:1500). Primary antibodies were detected by goat anti-rat Fab2 Cy3-coupled (Jackson ImmunoResearch, Europe) and goat anti-mouse Fab2 Alexa488-coupled secondary antibodies (Life technologies, 1:500). Fibers were examined and images captured using LSM 710 with ZEN 2009 software (Zeiss). CldU (red) and IdU (green) tracks were measured using LSM Image Browser (Zeiss) and μm values were converted into kilo base pairs. At least 150 forks were analysed from 3 repetitions. DNA fiber structures from 3 independent experiments were counted in ImageJ using the Cell Counter function.

Clonogenic survival

In colony formation assays, glioblastoma cells growing in the log phase were used. Cells ($n=400$ for LN229 and LN308, $n=800$ for U87) were seeded in duplicate in 60 mm Petri dishes. They were allowed to attach, exposed to 10 μM CCNU for 1 h, and then the medium was changed with/without addition of inhibitor. Cells were further incubated. After 7–10 d, the colonies were fixed with 70% ethanol for 10 min, stained in crystal-violet solution (1g/l dH_2O) for 10 min and colonies containing at least 40 cells were counted and presented graphically as a percentage of untreated cells (control). All colony assays were repeated at least three times.

Induction of apoptosis and necrosis

In order to distinguish between early stages of apoptosis and late apoptosis/necrosis, we used annexin V/propidium iodide (AV/PI) double staining of non-fixed cells as previously described [25]. Briefly, the culture medium of untreated or treated cells was collected, then the cells were washed in PBS and detached by trypsin/EDTA, added to the culture medium and centrifuged. The cell pellets were washed two times with PBS and suspended in 50 μl Annexin-binding buffer (Miltenyi Biotec). Annexin V-FITC from Miltenyi Biotec (2.5 μl) was added to each sample. After 15 min incubation on ice in the dark, 430 μl binding buffer and 1 $\mu\text{g/ml}$ PI were added. The flow cytometric measurement was carried out using FACS Canto II System (BD Biosciences). For each sample 10,000 cells were scored. The percentage of the

total induced cell death and the ratio between apoptosis and necrosis in mock-treated and CCNU resp. inhibitor treated samples was determined by using FACS Diva software (BD Bioscience). All results represent means of at least three independent experiments \pm SD.

Pancaspase inhibitor assay

Additionally to cell death determination we analyzed caspase activation *via* flow cytometry as previously described [48] with slight modifications. To this end we used the cell-permeable fluoromethyl ketone (FMK)-derived peptide zVAD-FMK, which binds covalently to the catalytic site of caspase proteases and acts as an effective irreversible general caspase inhibitor without additional cytotoxic effects. Briefly, harvested cells were re-suspended in 250 μ l PBS and incubated for 60 min in the presence of 20 μ M of FITC coupled-zVAD-FMK (CaspACETMFITC-VAD-FMK, Promega, Mannheim, Germany) in the incubator. Following incubation, cells were rinsed twice in cold phosphate buffered saline (PBS), fixed with ice-cold 70% ethanol and stored at -20°C for at least 2 h. Prior to flow cytometry, cells were digested in RNase A (0.03 mg/ ml PBS, 1 h, RT), counterstained with PI (16.5 μ g/ ml) and stored on ice until measurement. A total of 10.000 events were acquired and analyzed with FACS Diva software (BD Bioscience). Percentage of cells in the different phases of the cell cycle or in the subG1 fraction was determined on the basis of the DNA content using FACS Diva software (BD Bioscience). The percentage of cells with activated caspases (FITC-positive cell subpopulation) was determined by the same software. The results represent means of at least three independent experiments \pm SD.

Immunofluorescence

Cells grown on pre-cleaned cover slips were treated with CCNU and/or inhibitors. Following post-treatment incubation, the cells on the cover slips were fixed with ice-cold methanol/acetone (7:3, v/v) for 10 min at -20°C at the indicated time points. Following rehydration in PBS, the fixed cells were blocked/permeabilized in 10% normal goat serum +0.25% Triton-X100 in PBS for 1h. Further, the preparations were incubated with primary antibodies: mouse anti-phospho-H2AX (Ser139), anti-RPA2 from Merck Millipore (Germany) and rabbit monoclonal anti-phospho H2AX (Ser139) from Cell Signaling Technology. We used secondary anti-mouse and anti-rabbit antibodies coupled with Alexa Fluor 488 (Life technologies) or Cy3 (Jackson ImmunoResearch Europe). Nuclei were counterstained with DAPI containing Vectashield mounting medium (Vector Labs) for Metafer and To-Pro-3 for LSM microscopy. The slide-scanning platform Metafer (MetaSystems, Altlußheim, Germany) was used with Metafer4 software for automatic capture of images. Scoring of foci on captured images was performed with ImageJ software with suitable batch-macros as described [49]. Representative confocal images were captured by ZEN2009 software for

laser-scanning microscope LSM710 (Carl Zeiss). EdU (5-ethynyl-2'-deoxyuridine) incorporation for detection of S-phase cells was performed using the EdU Click-It Imaging Kit (Thermo Fisher Scientific) and FAM-azide click-it dye (Lumiprobe, Hannover, Germany). The intensity of the Click-It fluorescent dye bound to EdU in the DNA of EdU-labeled cells was measured onto LSM images by ZEN 2009 Software. EU (5-ethynyl-2'-uridine) incorporation for analysis of transcription rate was performed using the Click-iT® RNA Alexa Fluor 488 Imaging Kit (Thermofisher Scientific). The intensity of the Click-It fluorescent dye bound to EU was measured for each cell captured onto LSM images using the ImageJ software.

Western blotting

Protein extracts were prepared from LN229 cells following 1 h treatment with 30 μ M CCNU and post-treatment with 10 μ M B02, 25 μ M mirin or 20 μ M RI-1. Cells were detached from the dishes by trypsin/EDTA treatment and collected by centrifugation. The cell pellets were lysed, boiled in loading buffer at 95°C for 5 min and then cooled on ice for 5 min. Per slot, 30 μ g protein was loaded onto 5% SDS stacking gel/7.5, 10 or 15% separation gel (19:1, stock polyacrylamide: bisacrylamide) and run at 40 mA until the loading buffer indicator leaves the gel. Proteins were blotted onto a nitrocellulose membrane. Membranes were blocked for 1 h at room temperature in 5% (wt/v) albumin fraction of bovine serum in TBS containing 0.1% Tween (TBST), then washed two times in TBST and then incubated overnight at 4°C with the primary antibody, i.e. anti-H2AX (phospho-Ser139, 1:10,000) from Millipore-Merck; rabbit monoclonal anti-cleaved PARP (1:100,000) from Abcam; rabbit anti-p53 (phospho-Ser15), anti-H2AX (phospho-Ser139) and rabbit monoclonal anti-PTEN (1:1000) from Cell Signaling. After washing in TBST, the membranes were incubated with a donkey IRDye 800CW or IRDye 680 anti-mouse or anti-rabbit secondary antibody (1:10,000-1:25,000 from LI-COR Biosciences, Bad Homburg, Germany), dried and imaged by Odyssey v3.0 of the infrared imaging device Odyssey (LI-COR Biosciences, Bad Homburg, Germany). The mouse anti- β -actin (Santa Cruz) was used as a loading control (1:3000) followed by a secondary anti-mouse antibody.

Chromosome aberration (CA) analysis

Cells grown in 4 ml medium in 60 mm petri dishes were treated with 15 μ M CCNU for 60 min 1 cell cycle prior to fixation because we expected CA induction during the S-phase of the treatment cell cycle. Demecolcine (150 ng/ml) was added 2 h before harvest. Chromosome preparations were done according to standard protocols. Briefly, cells were harvested by trypsin:EDTA treatment, pelleted and resuspended in pre-warmed 0.075 M KCl and incubated for 10 min. Cells were pelleted and fixed 3 times in ice-cold methanol/acetic acid (3:1, v/v) mixture. The fixed cells were resuspended in a small volume of freshly prepared

ice-cold fixative, dropped onto pre-cleaned wet ice-cold slides. After being air-dried, the slides were stained in 5% phosphate buffered Giemsa solution. Fifty metaphases were evaluated per treatment level for chromosomal aberrations. The following aberrations were counted: chromatid breaks, chromatid translocations (triradials, quadriradials) and intercalary deletions. Gaps were not included in the final evaluation. Because of the variable numbers of chromosomes in the different cell lines used in this study, aberration frequencies were expressed as aberrations per chromosome and aberrations per metaphase (normalized to mean number of chromosomes for 50 metaphases of each treatment variant). Induced aberration frequencies for combined treatments in 100 metaphases were calculated by subtraction of the aberration frequency induced by HRi alone and compared to CCNU treatment alone.

Animal experiments

The animal experiments were approved by the government of Rhineland-Palatinate and the Animal Care and Use Committee of the University Medical Center Mainz and performed according to the federal law (Animal Protection Act of Germany). Immuno-deficient mice (Balb c, nu/nu, Janvier Labs, France) were housed in a sterile environment and allowed free access to food and water. Animals were 3-4 months of age at the start of the experiment. Tumor cells were injected subcutaneously over both flanks with 2.5×10^6 U87MG cells per flank. The animals were checked every other day to evaluate their health condition and tumor growth. When the tumors reached an average diameter of about 5 mm, the animals were divided into groups of 5 animals that were subjected to different treatments: to the animals of 1st group (vehicle control) corn oil (Sigma-Aldrich) alone was administered i. p.; 2nd group CCNU (25 µg/kg body weight diluted in 50 µl corn oil) was injected i. p., the 3rd group was treated i.p. with 50 mg/kg RI-1 diluted in 50 µl corn oil and the 4th group with the combination CCNU+RI-1. The health state, body weight and tumor growth were followed for 4 weeks until palpable tumors appeared. Tumor size was determined twice a week and tumor volumes were calculated using the formula $V_t = l \times b \times 0.5b$, where V_t is the tumor volume, l is the length and b the width of the tumour.

Statistics

We used the software GraphPad Prism version 5.00 for Windows by GraphPad Software (San Diego California USA) for statistical analyses. Data sets from three independent experiments were compared by one-tailed unpaired t-test or by unpaired t-test with Welch's correction (if variances between the data sets were significantly different). For chromosomal aberrations, the data on CCNU treated cells with/without posttreatment with HRi from three

independent experiments were compared by the non-parametric Mann-Whitney test. Tumor growth curves were compared by the Mann-Whitney test as well.

Results

CCNU induces ICLs in glioblastoma cells in the absence of MGMT activity

We used three well-established glioblastoma cell lines deficient in MGMT activity as an *in vitro* model [50]. The cell lines differ in their p53 status: LN229 and U87MG are p53 wild-type and LN308 is p53 mutated. Consequently, following treatment with ACNU or CCNU, p53 was phosphorylated (at serine 15) in LN229 and U87MG, whereas LN308 did not show phosphorylation of p53 (Fig. 1A). The lines differ also in their PTEN (phosphatase and tensin homolog) status; LN229 is PTEN wild-type, while LN308 and U87MG are PTEN deficient (Fig. 1A). Using a modified alkaline comet assay for the detection of crosslinks, we observed that CCNU treatment leads to the formation of ICLs in glioblastoma cells. Thus, as shown in Fig. 1B, the tail intensity was significantly reduced in the irradiated cell lines pretreated with 50 μ M CCNU, indicating the induction of ICLs.

To prove that the repair inhibitors B02, mirin and RI-1 are effective in the glioblastoma lines used here, we applied a plasmid-based repair assay. In cells transfected with pDRGFP a DSB was generated in the plasmid sequence by I-SceI, and the repair of the DSB by HR leads to GFP expression. As shown in Fig. 1C, the HR capacity observed in the control was significantly reduced following B02, mirin and RI-1 treatment. In contrast, DNA-PK inhibition caused a strong increase in the number of GFP positive cells, probably due to a compensatory enhancement of HR activity in the absence of the competitive NHEJ DSB repair pathway [46].

Effect of CCNU and HRi on DNA replication

Further, we investigated whether O^6 CIG mediated ICLs, which were induced at the dose levels applied in the subsequent inhibitor experiments, block DNA replication. To this end, we analysed the incorporation of the thymidine analogue EdU in the DNA following CCNU treatment. Representative images of EdU incorporation are shown in Fig. 2A. The quantification shows that 6 h after pulse-treatment (60 min) with CCNU the EdU incorporation was not significantly reduced (Fig. 2B) while 16 h later a significant reduction was observed (Fig. 2C). The HR inhibitors themselves had a replication-inhibiting effect 16 h after treatment. The inhibitors B02 and mirin given together with CCNU had no significant impact on EdU incorporation as measured 6 h after CCNU, but slightly ameliorated the effect 16 h later, while RI-1 did not (Fig. 2C).

To gain insight into the mechanism of replication inhibition, we made use of the DNA fiber labeling technique, where the DNA replication tracks are visualized through the detection of incorporated thymidine analogues. The distribution of the DNA fiber structures (defined in Fig. 2D together with representative images) showed an increase in the frequency of stalled replication forks (replication interrupted during the first CldU pulse; red segments in the columns) at 6 and 16 h after CCNU treatment, with an exacerbated effect 16 h after treatment. The HR inhibitors alone had an impact on ongoing replication, which was ameliorated if applied together with CCNU. Interestingly, RI-1 abrogated the effect of CCNU if measured 16 h after treatment (Fig. 2E and 2F). Overall, the data support the notion that at the dose level used here (resulting in moderate toxicity) CCNU-induced DNA lesions, very likely ICLs, only modestly inhibit replication and that the inhibitors B02 and mirin, but not RI-1, ameliorate the replication-blocking effect of CCNU.

Formation of RPA at stalled replication forks

CCNU is a potent inducer of RPA (replication protein A) foci (see Fig. 3A for representative images), which are considered as a marker of replication stress [51]. The quantitative analysis showed that high levels of RPA foci were induced in LN229 cells 24 h after pulse-treatment with 30 μ M CCNU (Fig. 3B). After 72 h the amount of RPA foci declined to nearly control level, indicating that damage repair has occurred. Similar numbers of RPA foci/cell were induced 24 h after combined treatments with CCNU plus either one of the inhibitors, however no significant decline was observed at 72 h (Fig. 3B). This indicates that RPA-inducing lesions are formed, but not repaired if cells are treated with CCNU followed by mirin or an inhibitor of HR.

Formation of DSBs after CCNU treatment and HR inhibition

Next, we analyzed DSBs formed following CCNU pulse treatment with and without post exposure to the HR inhibitors RI-1 and B02, and the MRE11 inhibitor mirin. In Fig. 4A, representative examples are shown of γ H2AX foci induced in LN229 cells 16 h after treatment (for examples of 6 h measure points see Supplement Fig. S2) and Fig. 4 C presents their quantification. The data demonstrate that a low number of DSB are formed 6 h after CCNU treatment and the inhibitors enhanced significantly their level. Following CCNU only, the DSB frequency is higher 16 h than 6 h after CCNU pulse-treatment and again the presence of inhibitors clearly enhanced their level. The data suggest that inhibition of HR and MRE11 ameliorates the DSB level.

In another experimental series γ H2AX foci were determined after longer times, i.e. 24 and 72 h after CCNU pulse-treatment, comparing the cell lines. Representative images for LN229, LN308 and U87MG are shown in Fig. 5A. The quantification revealed that high γ H2AX foci

levels were induced 24 h after CCNU pulse-treatment or the combined treatments with the inhibitors. At 72 h, the cells repaired most of the CCNU-induced DSBs. However, in the presence of the inhibitors the γ H2AX foci level did not decline, indicating DSBs induced by CCNU were not repaired (Fig. 5 panels B, C and D). To confirm the data, we analyzed the level of phosphorylated γ H2AX in Western blots. The experiments showed an increase in γ H2AX protein level after CCNU treatment alone. Following treatment with CCNU together with B02, mirin or RI-1 the initial level was the same (24 h after the begin of treatment), but the levels 48 and 72 h after treatment were clearly higher in the combined treatments than in the control CCNU only. The strongest effect was observed for B02 applied together with CCNU (Fig. 5E). The finding indicates that in the presence of B02, mirin and RI-1 DSBs induced by CCNU remained unrepaired, at least for a period of 48 h. In summary, the data shows that DSBs are formed in MGMT lacking glioblastoma cells treated with CCNU. These DSB are subject to repair. Inhibition of HR by B02 or RI-1 or targeting of MRE11 by mirin exerted an inhibitory effect on the repair of DSBs formed following CCNU treatment.

Increased levels of chromosomal aberrations in the presence of HR and MRE11 inhibitors

Next, we analysed the formation of CCNU-induced CA. The three glioblastoma cell lines used in our study differed in their karyotype: LN229 and LN308 were hypertriploid with ~82 and ~75 chromosomes per metaphase, respectively, whereas U87MG cells were diploid. Almost all cells displayed an aneuploidy karyotype (44-47 chromosomes per metaphase). We could show a significant increase of CCNU-induced structural CA after Rad51 inhibition with RI-1 and with B02 in all cell lines (Fig. 6A-C). For mirin, we observed a sensitizing effect only in LN308 (Fig. 6B). Under the same conditions (using the same concentrations of CCNU and HR inhibitors), the U87MG cells were much more resistant than LN229 and LN308 cells. The analysis of the aberration spectra revealed the predominant formation of chromatid-type aberrations, i.e. breaks and exchanges. The LN229 cells were very sensitive to Rad51 inhibition and especially after treatment with the combination of B0-2 and CCNU many multi-aberrant metaphases were observed with more than 50% of the chromosomes involved in complex rearrangements (see representative image in Fig. 6A) These data demonstrate the clastogenic effect of CCNU in glioblastoma cells, which is exacerbated if post-treatment occurred with either one of the inhibitors. In summary, we show that inhibition of Rad51 and MRE11 ameliorates the genotoxic effects of CCNU in glioblastoma cells.

Colony formation and induced apoptosis/necrosis after Rad51 and MRE11 inhibition

To explore the effect of HR and MRE11 inhibitors on reproductive cell survival, we conducted colony forming assays. The data are shown in Fig. 7. We observed a significantly reduced

survival after CCNU followed by B02, mirin or RI-1 in LN229 cells (Fig. 7A), following B02 and RI-1 in LN308 cells (Fig. 7B) and following RI-1 in U87MG cells (Fig. 7C). Thus, the most consistent results as to enhancing reproductive cell death followed by CCNU was obtained for RI-1.

To further study the effect of the inhibitors on glioblastoma cell sensitivity, we used the AV/PI assay, measuring apoptosis and necrosis. The data shown in Fig. 7D-F demonstrate that CCNU-induced cell death by apoptosis and necrosis is ameliorated when CCNU was applied concomitantly with RI-1, mirin and B02 (Fig. 7D for LN229, Fig. 7E for LN308 and Fig. 7F for U87MG). Although both apoptosis and necrosis were induced, apoptosis was prevailing after CCNU treatment alone and after the combined treatments. The increased levels of apoptosis following treatment with the inhibitors were confirmed by caspase assays, showing a higher percentage of cells with activated caspases following treatment with CCNU plus HRi (Fig. 8 panels A, B, C for LN229, LN308 and U87MG, respectively). Apoptosis induced by CCNU was accompanied by PARP-1 cleavage (Fig. 8D), which was clearly higher after Rad51 inhibition by B02 and RI-1 in LN229 cells. Mirin alone induced already PARP1 cleavage, which is in line with its toxicity seen in other assays.

RI-1 ameliorates the anticancer effect of CCNU

Having shown that RI-1 is able to enhance CCNU-induced glioma cell death in a nearly non-toxic dose range *in vitro*, we investigated the toxicity of RI-1 *in vivo* alone and in combination with CCNU in a nude mouse xenograft model. Administration of RI-1 did not result in changes in the health status or body weight during a 3-week post-exposure period (data not shown). Representative images of U87MG tumor xenografts are shown in Fig. 9A, demonstrating the impressive effect of combination treatment CCNU plus RI-1. The tumor growth was quantified, revealing that CCNU treatment leads to a reduction in tumor size which is greatly ameliorated if CCNU is combined with RI-1 (Fig. 9B). Fig. 9C shows body weight of the mice in the different treatment groups, which was not clearly impaired in the combination treatment setting. The data let us conclude that the combined treatment CCNU plus RI-1 is tolerable and has an advantage over CCNU alone as to inhibition of tumor growth in the xenograft model.

Discussion

This study was aimed at analysing whether inhibition of homologous recombination or inhibition of MRE11 results in an enhancement of the killing effect of CCNU, which is a

representative of CNUs used in glioblastoma therapy. We show that the inhibitors RI-1 and B02, which target Rad51, enhance the level of DSBs and chromosomal aberrations and ameliorate the killing effect of CCNU in glioblastoma cells. The same was observed for mirin, which targets MRE11, a component of the MRN complex.

CCNU, like other chloroethylating agents, alkylates DNA at several sites [52], including the O^6 -position of guanine. Intramolecular rearrangement of O^6 -chloroethylguanine gives rise to ICLs between guanine and cytosine. Since MGMT, which repairs O^6 -chloroethylguanine, nearly completely abolishes the cytotoxicity of CNUs, at least in the pharmacologically low dose range [25], it can be extrapolated that this minor damage, O^6 -chloroethylguanine and the subsequently formed ICLs, are responsible for the genotoxicity and the killing effect of CNUs. ICLs block DNA replication, which was observed in our experiments within the cytotoxic dose range measuring EdU incorporation at times when ICLs were formed (16 h following treatment). The inhibitory effect on EdU incorporation was, however, quite modest. This is likely the result of the small amount of ICLs induced in comparison to monoadducts. In the DNA fiber-labeling experiments we observed already 6 h after CCNU pulse-treatment an increase in the frequency of uniformly labeled tracks (only CldU or IdU incorporated), which likely represent blocked replication forks during the labeling period. Since blockage of fork movement results in stalled replication forks, replication fork collapse and finally DSBs according to a mechanism described for other genotoxic insults like UV or MMS [53, 54], we posit that the same mechanism takes place following CCNU-induced DNA adducts, very likely ICLs. The significant formation of DSB at this early time-point and their further accumulation support this notion.

DSBs formed by alkylating agents are subject to repair by HR, as previously shown for both O^6 -methylguanine inducing anticancer drugs [55, 56] and chloroethylating agents [25, 55, 57]. Therefore, it was reasonable to hypothesize that inhibition of HR ameliorates DSB formation. The data presented here can be taken to confirm that this is indeed the case. Whereas without HR inhibition the level of γ H2AX declined 72 h after formation, they remained at a high level in RI-1 and B02 post-treated cells. This was associated with a significant increase in chromosomal changes and killing effects, notably by the induction of apoptosis. RI-1 binds directly to human RAD51 at cysteine-319 [42]. For B02, a specific binding to the Rad51 protein was also demonstrated, but the exact binding site was not identified [39]. In each case, the binding of Rad51 to single-stranded DNA becomes more difficult, which inflicts on the HR process. Comparing the inhibitors, we observed that RI-1 is less cytotoxic than B02 in glioblastoma cells and, overall, slightly more efficient in enhancing CCNU-induced genotoxicity and cell death.

Another goal of this work was to compare pharmacological inhibitors of HR with an inhibitor of DNA damage signaling, mirin. The MRN complex plays a profound role in the recognition of DSBs. MRE11 is a key protein in the trimeric MRN complex, composed of NBS1, RAD50 and MRE11. MRE11 contains a core phosphodiesterase domain that is responsible for its multiple nuclease activities in a single endo/exonuclease mechanism [58]. Mirin was shown to bind to MRE11 and to inhibit its nuclease activity without affecting MRE11 binding to DNA or the MRN associated DNA-tethering activity [38]. In addition, it inhibits the ATM-dependent phosphorylation of NBS1 and CHK2 [38]. Therefore, the activation of the ATM/ATR-CHK1-CHK2 pathway cannot be triggered in a proper way. Since MRN and ATM operate independently in the recognition of DNA damage and processing of DSBs for HR repair [59], it was hypothesized that the pharmacological inhibition of the MRN complex exerts a sensitizing effect similar to what we observed with Rad51 inhibitors. This was indeed the case since mirin ameliorated the level of DSBs, aberrations and apoptosis/necrosis in CCNU-treated glioblastoma cells similar to Rad51 inhibitors. We should note that a combined treatment with mirin and Rad51i was heavily toxic for the cells.

Previously it was shown that downregulation of Rad51 or BRCA2 by means of siRNA enhances the killing response of glioblastoma cells treated with temozolomide or CCNU [55, 57]. On principle, virus-mediated transducing systems might represent a reasonable approach for targeting HR in glioblastoma therapy. However, it is clear that viral transduction strategies are more difficult in finding their way to the clinic than pharmacological inhibitors. Therefore, we favor the use of HR inhibitors as a strategy for enhancing the effect of alkylating drugs in glioma therapy. When comparing the inhibitors used in this study, we observed for B02 and for mirin an inhibiting effect on transcription, which might impact the survival of non-cancer cells. RI-1 on the other hand did not affect transcription (Supplement Fig. S3) and, therefore, might have less side effects on non-target tissues. Actually, RI-1 was well tolerated in the *in vivo* setting and potent in ameliorating the cytotoxic and antitumor activity of CCNU, as shown in the U87MG xenograft model. It is clear that clinical safety trials are needed for assessing the systemic toxicity of the drugs. Although the RAD51 inhibitors have been around for a number of years [60] they have not yet moved to extended clinical trials very likely because of supporting preclinical data were lacking. This study hopefully encourages the application of HR inhibitors in trials assessing their effect in combination with alkylating drugs that are used in the therapy of glioblastomas and other tumor groups.

Acknowledgements

We thank Anna Frumkina and Georg Nagel for technical assistance. We are very grateful to Ann Parplys for critical reading and helpful comments on the manuscript.

References

1. Patel MA, Kim JE, Ruzevick J, Li G, Lim M: The future of glioblastoma therapy: synergism of standard of care and immunotherapy. *Cancers* 2014, 6(4):1953-1985.
2. Preusser M, de Ribaupierre S, Wohrer A, Erridge SC, Hegi M, Weller M, Stupp R: Current concepts and management of glioblastoma. *Ann Neurol* 2011, 70(1):9-21.
3. Stupp R, Hegi ME, Mason WP, van den Bent MJ, Taphoorn MJ, Janzer RC, Ludwin SK, Allgeier A, Fisher B, Belanger K *et al*: Effects of radiotherapy with concomitant and adjuvant temozolomide versus radiotherapy alone on survival in glioblastoma in a randomised phase III study: 5-year analysis of the EORTC-NCIC trial. *Lancet Oncol* 2009, 10(5):459-466.
4. Lee FY, Workman P, Roberts JT, Bleeher NM: Clinical pharmacokinetics of oral CCNU (lomustine). *Cancer chemotherapy and pharmacology* 1985, 14(2):125-131.
5. Glas M, Bahr O, Felsberg J, Rasch K, Wiewrodt D, Schabet M, Simon M, Urbach H, Steinbach JP, Rieger J *et al*: NOA-05 phase 2 trial of procarbazine and lomustine therapy in gliomatosis cerebri. *Ann Neurol* 2011, 70(3):445-453.
6. Glas M, Happold C, Rieger J, Wiewrodt D, Bahr O, Steinbach JP, Wick W, Kortmann RD, Reifenberger G, Weller M *et al*: Long-term survival of patients with glioblastoma treated with radiotherapy and lomustine plus temozolomide. *J Clin Oncol* 2009, 27(8):1257-1261.
7. Glas M, Hundsberger T, Stuplich M, Wiewrodt D, Kurzwelly D, Nguyen-Huu B, Rasch K, Herrlinger U: Nimustine (ACNU) plus teniposide (VM26) in recurrent glioblastoma. *Oncology* 2009, 76(3):184-189.
8. Glas M, Rasch K, Wiewrodt D, Weller M, Herrlinger U: Procarbazine and CCNU as initial treatment in gliomatosis cerebri. *Oncology* 2008, 75(3-4):182-185.
9. Gwak HS, Youn SM, Kwon AH, Lee SH, Kim JH, Rhee CH: ACNU-cisplatin continuous infusion chemotherapy as salvage therapy for recurrent glioblastomas: phase II study. *J Neurooncol* 2005, 75(2):173-180.
10. Weller M, Muller B, Koch R, Bamberg M, Krauseneck P: Neuro-Oncology Working Group 01 trial of nimustine plus teniposide versus nimustine plus cytarabine chemotherapy in addition to involved-field radiotherapy in the first-line treatment of malignant glioma. *J Clin Oncol* 2003, 21(17):3276-3284.
11. Fu D, Calvo JA, Samson LD: Balancing repair and tolerance of DNA damage caused by alkylating agents. *Nat Rev Cancer* 2012, 12(2):104-120.
12. Ludlum DB: DNA alkylation by the haloethylnitrosoureas: nature of modifications produced and their enzymatic repair or removal. *Mutat Res* 1990, 233(1-2):117-126.
13. Kaina B, Christmann M, Naumann S, Roos WP: MGMT: key node in the battle against genotoxicity, carcinogenicity and apoptosis induced by alkylating agents. *DNA Repair (Amst)* 2007, 6(8):1079-1099.
14. Bobola MS, Tseng SH, Blank A, Berger MS, Silber JR: Role of O6-methylguanine-DNA methyltransferase in resistance of human brain tumor cell lines to the clinically relevant methylating agents temozolomide and streptozotocin. *Clin Cancer Res* 1996, 2(4):735-741.
15. Kaina B, Fritz G, Mitra S, Coquerelle T: Transfection and expression of human O6-methylguanine-DNA methyltransferase (MGMT) cDNA in Chinese hamster cells: the role of MGMT in protection against the genotoxic effects of alkylating agents. *Carcinogenesis* 1991, 12(10):1857-1867.

16. Preuss I, Haas S, Eichhorn U, Eberhagen I, Kaufmann M, Beck T, Eibl RH, Dall P, Bauknecht T, Hengstler J *et al*: Activity of the DNA repair protein O6-methylguanine-DNA methyltransferase in human tumor and corresponding normal tissue. *Cancer Detect Prev* 1996, 20(2):130-136.
17. Preuss I, Thust R, Kaina B: Protective effect of O6-methylguanine-DNA methyltransferase (MGMT) on the cytotoxic and recombinogenic activity of different antineoplastic drugs. *Int J Cancer* 1996, 65(4):506-512.
18. Christmann M, Nagel G, Horn S, Krahn U, Wiewrodt D, Sommer C, Kaina B: MGMT activity, promoter methylation and immunohistochemistry of pretreatment and recurrent malignant gliomas: a comparative study on astrocytoma and glioblastoma. *Int J Cancer* 2010, 127(9):2106-2118.
19. Christmann M, Verbeek B, Roos WP, Kaina B: O(6)-Methylguanine-DNA methyltransferase (MGMT) in normal tissues and tumors: enzyme activity, promoter methylation and immunohistochemistry. *Biochim Biophys Acta* 2011, 1816(2):179-190.
20. Stupp R, Hegi ME, van den Bent MJ, Mason WP, Weller M, Mirimanoff RO, Cairncross JG, European Organisation for R, Treatment of Cancer Brain T, Radiotherapy G *et al*: Changing paradigms--an update on the multidisciplinary management of malignant glioma. *The oncologist* 2006, 11(2):165-180.
21. Vare D, Groth P, Carlsson R, Johansson F, Erixon K, Jenssen D: DNA interstrand crosslinks induce a potent replication block followed by formation and repair of double strand breaks in intact mammalian cells. *DNA Repair (Amst)* 2012, 11(12):976-985.
22. Muniandy PA, Liu J, Majumdar A, Liu ST, Seidman MM: DNA interstrand crosslink repair in mammalian cells: step by step. *Crit Rev Biochem Mol Biol* 2010, 45(1):23-49.
23. Sengerova B, Wang AT, McHugh PJ: Orchestrating the nucleases involved in DNA interstrand cross-link (ICL) repair. *Cell Cycle* 2011, 10(23):3999-4008.
24. Brozovic A, Damrot J, Tsaryk R, Helbig L, Nikolova T, Hartig C, Osmak M, Roos WP, Kaina B, Fritz G: Cisplatin sensitivity is related to late DNA damage processing and checkpoint control rather than to the early DNA damage response. *Mutat Res* 2009, 670(1-2):32-41.
25. Nikolova T, Hennekes F, Bhatti A, Kaina B: Chloroethylnitrosourea-induced cell death and genotoxicity: cell cycle dependence and the role of DNA double-strand breaks, HR and NHEJ. *Cell Cycle* 2012, 11(14):2606-2619.
26. Chapman JR, Taylor MR, Boulton SJ: Playing the end game: DNA double-strand break repair pathway choice. *Mol Cell* 2012, 47(4):497-510.
27. Thompson LH: Recognition, signaling, and repair of DNA double-strand breaks produced by ionizing radiation in mammalian cells: the molecular choreography. *Mutat Res* 2012, 751(2):158-246.
28. Iliakis G, Wang H, Perrault AR, Boecker W, Rosidi B, Windhofer F, Wu W, Guan J, Terzoudi G, Pantelias G: Mechanisms of DNA double strand break repair and chromosome aberration formation. *Cytogenet Genome Res* 2004, 104(1-4):14-20.
29. Holthausen JT, Wyman C, Kanaar R: Regulation of DNA strand exchange in homologous recombination. *DNA Repair (Amst)* 2010, 9(12):1264-1272.
30. Majka J, Alford B, Ausio J, Finn RM, McMurray CT: ATP hydrolysis by RAD50 protein switches MRE11 enzyme from endonuclease to exonuclease. *J Biol Chem* 2012, 287(4):2328-2341.
31. Ying S, Hamdy FC, Helleday T: Mre11-dependent degradation of stalled DNA replication forks is prevented by BRCA2 and PARP1. *Cancer Res* 2012, 72(11):2814-2821.
32. Connell PP, Jayathilaka K, Haraf DJ, Weichselbaum RR, Vokes EE, Lingen MW: Pilot study examining tumor expression of RAD51 and clinical outcomes in human head cancers. *International journal of oncology* 2006, 28(5):1113-1119.
33. Maacke H, Jost K, Opitz S, Miska S, Yuan Y, Hasselbach L, Luttes J, Kalthoff H, Sturzbecher HW: DNA repair and recombination factor Rad51 is over-expressed in human pancreatic adenocarcinoma. *Oncogene* 2000, 19(23):2791-2795.

34. Maacke H, Opitz S, Jost K, Hamdorf W, Henning W, Kruger S, Feller AC, Lopens A, Diedrich K, Schwinger E *et al*: Over-expression of wild-type Rad51 correlates with histological grading of invasive ductal breast cancer. *Int J Cancer* 2000, 88(6):907-913.
35. Qiao GB, Wu YL, Yang XN, Zhong WZ, Xie D, Guan XY, Fischer D, Kolberg HC, Kruger S, Stuerzbecher HW: High-level expression of Rad51 is an independent prognostic marker of survival in non-small-cell lung cancer patients. *Brit J Cancer* 2005, 93(1):137-143.
36. Tennstedt P, Fresow R, Simon R, Marx A, Terracciano L, Petersen C, Sauter G, Dikomey E, Borgmann K: RAD51 overexpression is a negative prognostic marker for colorectal adenocarcinoma. *Int J Cancer* 2013, 132(9):2118-2126.
37. Welsh JW, Ellsworth RK, Kumar R, Fjerstad K, Martinez J, Nagel RB, Eschbacher J, Stea B: Rad51 protein expression and survival in patients with glioblastoma multiforme. *Int J Radiat Oncol Biol Phys* 2009, 74(4):1251-1255.
38. Dupre A, Boyer-Chatenet L, Sattler RM, Modi AP, Lee JH, Nicolette ML, Kopelovich L, Jasin M, Baer R, Paull TT *et al*: A forward chemical genetic screen reveals an inhibitor of the Mre11-Rad50-Nbs1 complex. *Nat Chem Biol* 2008, 4(2):119-125.
39. Huang F, Mazina OM, Zentner IJ, Cocklin S, Mazin AV: Inhibition of homologous recombination in human cells by targeting RAD51 recombinase. *J Med Chem* 2012, 55(7):3011-3020.
40. Huang F, Motlekar NA, Burgwin CM, Napper AD, Diamond SL, Mazin AV: Identification of specific inhibitors of human RAD51 recombinase using high-throughput screening. *ACS Chem Biol* 2011, 6(6):628-635.
41. Budke B, Kalin JH, Pawlowski M, Zelivianskaia AS, Wu M, Kozikowski AP, Connell PP: An Optimized RAD51 Inhibitor That Disrupts Homologous Recombination without Requiring Michael Acceptor Reactivity. *J Med Chem* 2013, 56(1):254-263.
42. Budke B, Logan HL, Kalin JH, Zelivianskaia AS, Cameron McGuire W, Miller LL, Stark JM, Kozikowski AP, Bishop DK, Connell PP: RI-1: a chemical inhibitor of RAD51 that disrupts homologous recombination in human cells. *Nucleic Acids Res* 2012, 40(15):7347-7357.
43. Switzeny OJ, Christmann M, Renovanz M, Giese A, Sommer C, Kaina B: MGMT promoter methylation determined by HRM in comparison to MSP and pyrosequencing for predicting high-grade glioma response. *Clinical epigenetics* 2016, 8:49.
44. Usanova S, Piee-Staffa A, Sied U, Thomale J, Schneider A, Kaina B, Koberle B: Cisplatin sensitivity of testis tumour cells is due to deficiency in interstrand-crosslink repair and low ERCC1-XPF expression. *Mol Cancer* 2010, 9:248.
45. Lips J, Kaina B: DNA double-strand breaks trigger apoptosis in p53-deficient fibroblasts. *Carcinogenesis* 2001, 22(4):579-585.
46. Robert F, Barbeau M, Ethier S, Dostie J, Pelletier J: Pharmacological inhibition of DNA-PK stimulates Cas9-mediated genome editing. *Genome medicine* 2015, 7(1):93.
47. Parplys AC, Petermann E, Petersen C, Dikomey E, Borgmann K: DNA damage by X-rays and their impact on replication processes. *Radiotherapy and oncology : journal of the European Society for Therapeutic Radiology and Oncology* 2012, 102(3):466-471.
48. Goldstein M, Roos WP, Kaina B: Apoptotic death induced by the cyclophosphamide analogue mafosfamide in human lymphoblastoid cells: contribution of DNA replication, transcription inhibition and Chk/p53 signaling. *Toxicol Appl Pharmacol* 2008, 229(1):20-32.
49. Nikolova T, Dvorak M, Jung F, Adam I, Kramer E, Gerhold-Ay A, Kaina B: The gammaH2AX assay for genotoxic and nongenotoxic agents: comparison of H2AX phosphorylation with cell death response. *Toxicol Sci* 2014, 140(1):103-117.
50. Hermisson M, Klumpp A, Wick W, Wischhusen J, Nagel G, Roos W, Kaina B, Weller M: O6-methylguanine DNA methyltransferase and p53 status predict temozolomide sensitivity in human malignant glioma cells. *J Neurochem* 2006, 96(3):766-776.

51. Murphy AK, Fitzgerald M, Ro T, Kim JH, Rabinowitsch AI, Chowdhury D, Schildkraut CL, Borowiec JA: Phosphorylated RPA recruits PALB2 to stalled DNA replication forks to facilitate fork recovery. *J Cell Biol* 2014, 206(4):493-507.
52. Scharer OD: DNA interstrand crosslinks: natural and drug-induced DNA adducts that induce unique cellular responses. *Chembiochem* 2005, 6(1):27-32.
53. Federico MB, Vallerga MB, Radl A, Paviolo NS, Bocco JL, Di Giorgio M, Soria G, Gottifredi V: Chromosomal Integrity after UV Irradiation Requires FANCD2-Mediated Repair of Double Strand Breaks. *PLoS genetics* 2016, 12(1):e1005792.
54. Tercero JA, Diffley JF: Regulation of DNA replication fork progression through damaged DNA by the Mec1/Rad53 checkpoint. *Nature* 2001, 412(6846):553-557.
55. Quiros S, Roos WP, Kaina B: Rad51 and BRCA2--New molecular targets for sensitizing glioma cells to alkylating anticancer drugs. *PLoS One* 2011, 6(11):e27183.
56. Roos WP, Nikolova T, Quiros S, Naumann SC, Kiedron O, Zdzienicka MZ, Kaina B: Brca2/Xrcc2 dependent HR, but not NHEJ, is required for protection against O(6)-methylguanine triggered apoptosis, DSBs and chromosomal aberrations by a process leading to SCEs. *DNA Repair (Amst)* 2009, 8(1):72-86.
57. Kondo N, Takahashi A, Mori E, Noda T, Zdzienicka MZ, Thompson LH, Helleday T, Suzuki M, Kinashi Y, Masunaga S *et al*: FANCD1/BRCA2 plays predominant role in the repair of DNA damage induced by ACNU or TMZ. *PLoS One* 2011, 6(5):e19659.
58. Hopfner KP, Karcher A, Craig L, Woo TT, Carney JP, Tainer JA: Structural biochemistry and interaction architecture of the DNA double-strand break repair Mre11 nuclease and Rad50-ATPase. *Cell* 2001, 105(4):473-485.
59. Czornak K, Chughtai S, Chrzanowska KH: Mystery of DNA repair: the role of the MRN complex and ATM kinase in DNA damage repair. *J Appl Genet* 2008, 49(4):383-396.
60. Choy G, Joshi-Hangal R, Oganessian A, Fine G, Rasmussen S, Collier J, Kissling J, Sahai A, Azab M, Redkar S: Safety, tolerability, and pharmacokinetics of amuvatinib from three phase 1 clinical studies in healthy volunteers. *Cancer chemotherapy and pharmacology* 2012, 70(1):183-190.

Figure legends

Figure 1.

DNA repair in glioblastoma cells treated with CCNU. A, p53 and PTEN status of the cell lines LN229, LN308, U87MG. Treatment with ACNU or CCNU induces phosphorylation of p53 at serine 15 in LN229 and U87MG, but not in LN308 cells. LN229 expresses PTEN while LN308 and U87MG do not. B, modified alkaline comet assay for the detection of CCNU-induced cross-links in LN229, LN308 and U87MG. Treatment with 50 μ M CCNU leads to a significant reduction of tail intensity in the comets induced by 8 Gy irradiation due to the formation of ICLs, which do not allow migration of the fragmented DNA. Data from 3 independent experiments are shown and compared by two-tailed t-test, where ** $p < 0.01$, *** $p < 0.001$. C, homologous recombination activity was measured by quantification of GFP positive cells. Cells were non-treated or treated with one of the inhibitors: 10 μ M B02, 25 μ M mirin, 25 μ M RI-1 or 1 μ M KU0060648. The non-inhibitor treated control was set to 1. The representative FACS plots show the GFP-positive cell population (P2, green staining) upon transfection with pC β ASceI in the absence/presence of inhibitors. Data from 3 independent experiments were pooled and compared by t-test, ** $p < 0.01$, *** $p < 0.001$.

Figure 2: Effect of CCNU on DNA replication in the absence (Con) or presence of HRi. A to C, cells were treated with 30 μ M CCNU for 60 min followed by continuous HRi treatment and labelled with the thymidine analogues 6 or 16 h after the CCNU treatment. For concentrations of HR inhibitors see legend of Fig. 1C. The intensity of EdU staining of labelled cells was determined as described in M&M. A, Images of LN229 cells labelled with EdU 6 h after CCNU and HRi treatment. B, quantification of EdU incorporation 6 h after treatment. C, EdU incorporation 16 h after treatment. Data represent the mean of three independent experiments, ** $p < 0.01$, *** $p < 0.001$. D, schematic presentation of labelled DNA fibers and representative images of the corresponding DNA fiber structures. E, percent distribution of DNA fiber structures 6 h after CCNU/HRi treatment. F, percent distribution of DNA fiber structures measured 16 h after CCNU/HRi treatment.

Figure 3. Kinetics of formation and repair of RPA2 foci. A, representative confocal images of RPA2 foci in LN229 cells following treatment with CCNU and post-incubated with B02, mirin and R-1. Nuclei were counterstained with To-Pro-3 (blue). B, RPA2 foci/cell determined 24 and 72 h following treatment with CCNU (30 μ M, 60 min) of LN229 cells. Cells were not post-treated (control) or post-treated with B02, mirin or RI-1 using concentrations indicated in

legend of Fig. 1C. Data from 3 independent experiments were pooled and compared by t-test, * $p < 0.05$.

Figure 4. Kinetics of formation and repair of DSBs analysed by γ H2AX foci formation in LN229 glioblastoma cells. A, representative images of γ H2AX (red) foci 16 h after treatment, aptured by LSM; nuclei (blue) were stained with To-Pro-3. B, quantification; cells were treated with 30 μ M CCNU (60 min) without (Con) or with post-treatment with B02, mirin or RI-1 with concentrations indicated Fig. 1C. Data from three independent experiments were compared by t-test, * $p < 0.05$.

Figure 5. Formation and repair of DSBs analysed by γ H2AX foci formation ($\text{H2AX}_{\text{S139}}$) in LN229, LN308 and U87MG glioblastoma cells. A, representative images of γ H2AX (green) foci (captured by Metafer4). Nuclei (blue) were counterstained with To-Pro-3. B-D, induced γ H2AX foci measured 24 and 72 h after CCNU treatment of LN229 (B), LN308 (C) and U87MG (D) cells. Cells were treated with 30 μ M CCNU (60 min) without (Con) or with post-treatment with B02, mirin or RI-1 using concentrations indicated in legend of Fig. 1C. Data from 3 independent experiments were compared by t-test, * $p < 0.05$, ** $p < 0.01$. E, CCNU-induced phosphorylation of H2AX at serine 139 detected by Western blot analysis of total extracts from LN229 cells. Cells were harvested 24, 48 and 72 h after the onset of treatment with CCNU.

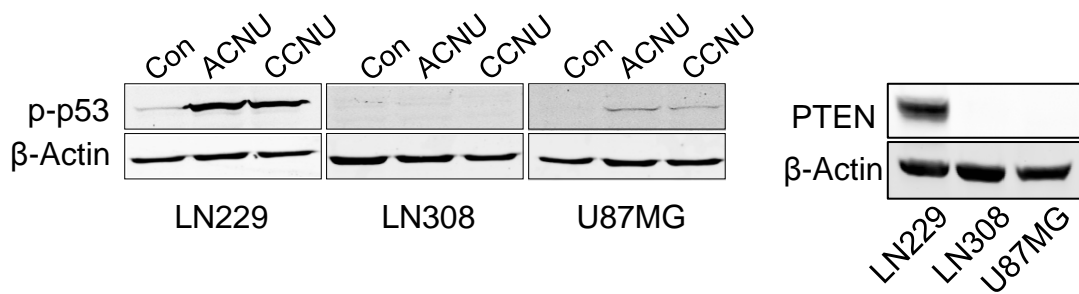
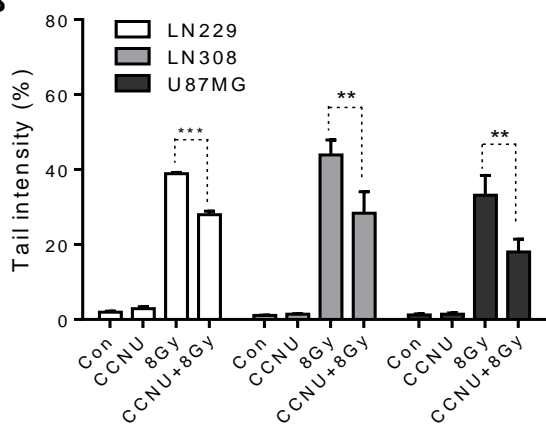
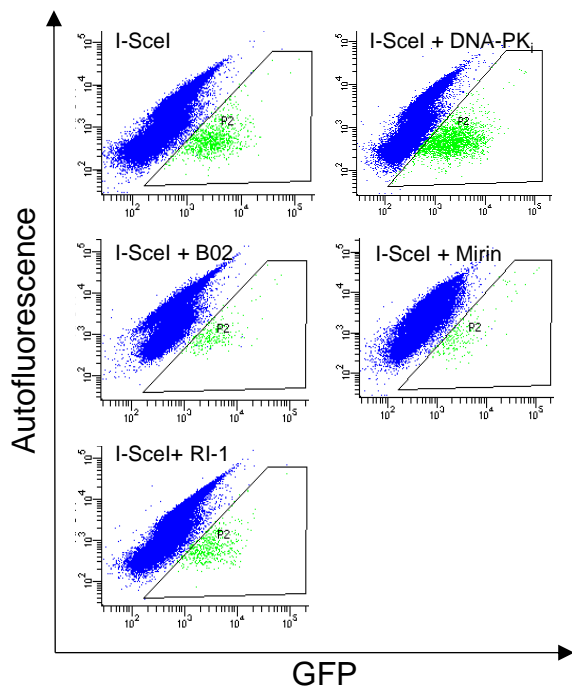
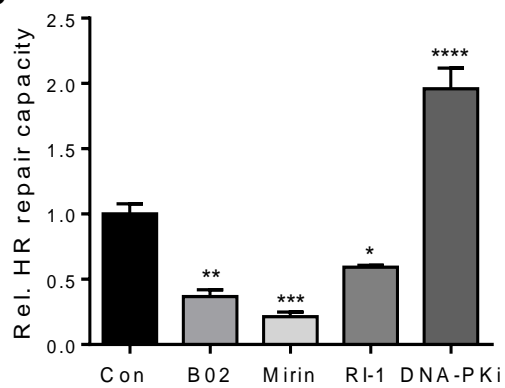
Figure 6. Effects of HRi on CCNU-induced chromosomal breakage in glioblastoma cells. Frequency of chromosomal aberrations per metaphase in LN229 (A), LN308 (B) and U87MG cells (C) treated with CCNU (15 μ M, 60 min) alone or post-treated with B02, mirin or RI-1 at concentrations indicated in legend of Fig. 1C. The right panels show representative images of metaphases with aberrations after treatment with 15 μ M CCNU followed by 10 μ M B02. Data from 3 independent experiments were compared by Mann-Whitney test (* $p \leq 0.05$).

Figure 7. Clonogenic survival and apoptosis and necrosis following CCNU and HRi treatment. (A-C) Clonogenic survival induced by CCNU in combination with HR inhibitors in glioblastoma cells: (A) LN229, (B) LN308 and (C) U87MG. Cells were treated with CCNU (10 μ M, 60 min) alone or post-treated with 2.5 μ M B02, 12.5 μ M mirin or 5 μ M RI-1, then incubated until colonies were formed, fixed and stained. Data from 3 independent experiments were pooled and compared by t-test, * $p < 0.05$, ** $p < 0.01$, *** $p < 0.001$. (D-F) Apoptosis/necrosis induced by CCNU in combination with HR inhibitors in glioblastoma cells: (D) LN229, (E) LN308 and (F) U87MG. Apoptosis and necrosis were determined by AV/PI after treatment of exponentially growing cells with CCNU (15 μ M, 60 min) followed by post-

treatment with HR-inhibitors. Concentrations of HR inhibitors were as in Fig. 1C. Means with S.D. of three independent experiments are shown and compared by t-test, * $p < 0.05$, ** $p < 0.01$, *** $p < 0.001$.

Figure 8. Caspase activation in (A) LN229, (B) LN308 and (C) U87MG cells 72 h after treatment with CCNU (30 μ M, 60 min) with or without post-treatment with HR-inhibitors (concentrations as indicated in legend Fig. 1C). Cells were harvested, incubated with FITC-coupled pan-caspase inhibitor, fixed, RNAase digested, stained with PI and counted by flow cytometry. Means with S.D. of three independent experiments are shown. D, CCNU-induced PARP cleavage in LN229 cells 48 h after the onset of treatment.

Figure 9. Tumor growth in a xenograft mouse model. Nude mice were inoculated with U87MG cells. Mice with palpable tumors received CCNU only (25 mg/kg b. w.), RI-1 only (50 mg/kg b. w.), CCNU + RI-1, or 50 μ l vehicle only (control). Tumor growth and body weight were determined in 4-day intervals. A, representative images of mice (control and treated) at the day of termination. B, tumor growth as a function of time. The relative tumor volume is expressed as increase of tumor volume from the day of CCNU treatment (which was set to 1) until termination of the experiment. At day 1 CCNU and RI-1 were administered. The mean tumor size with S.D. was determined from at least 5 mice per group bearing two tumors each. Significant difference between CCNU only and CCNU+RI-1 is indicated by asterisk. C, body weight determined in parallel with the tumour volume at the indicated time points and expressed as percentage of the body weight measured on the day of CCNU and/or HRI treatment.

A**B****C****Figure 1**

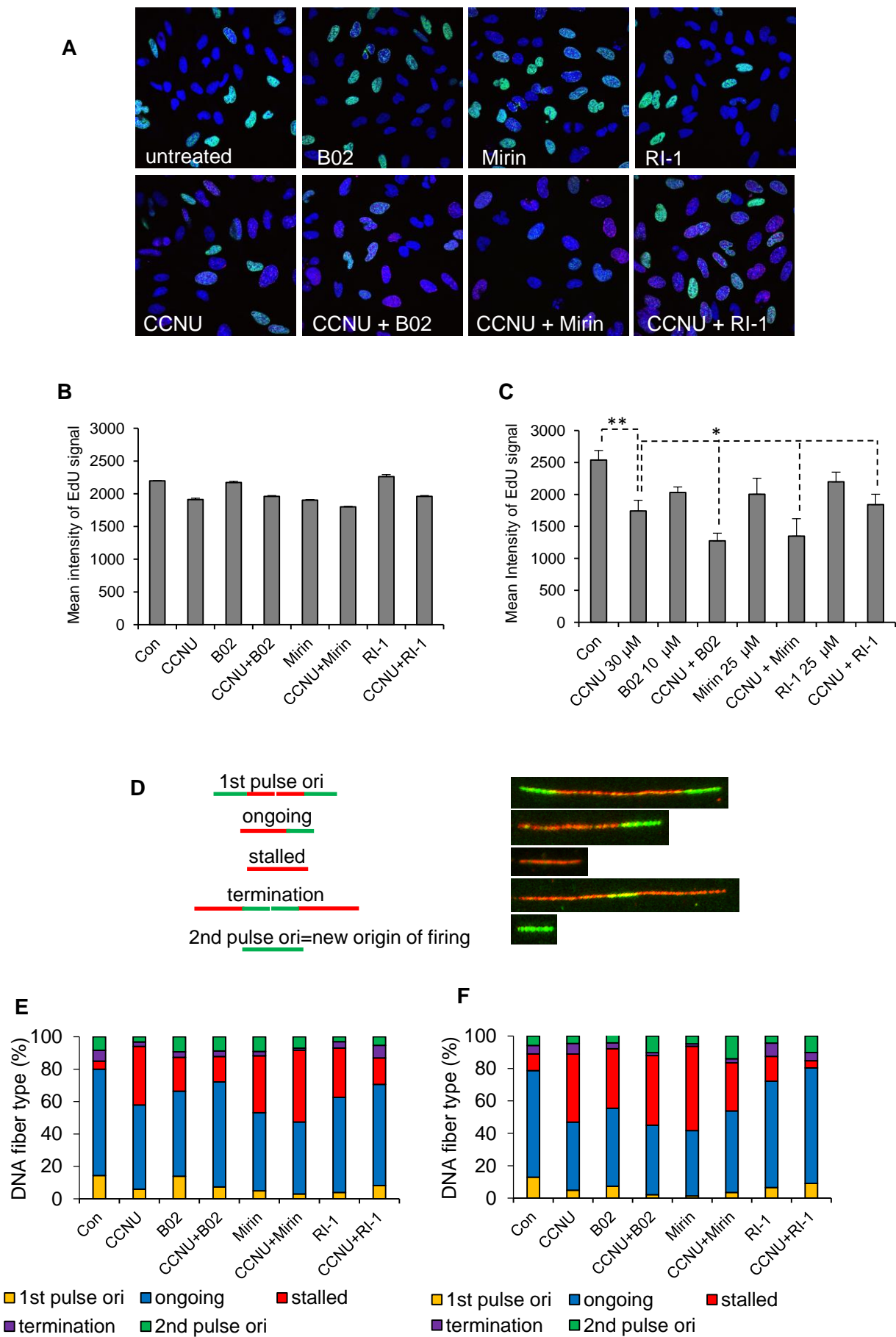
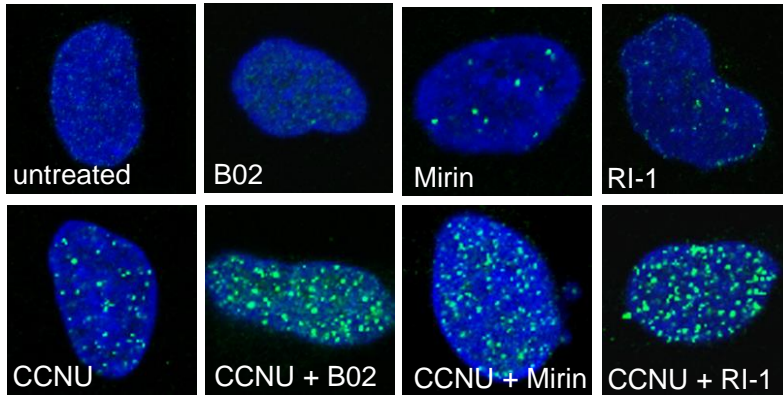


Figure 2

A



B

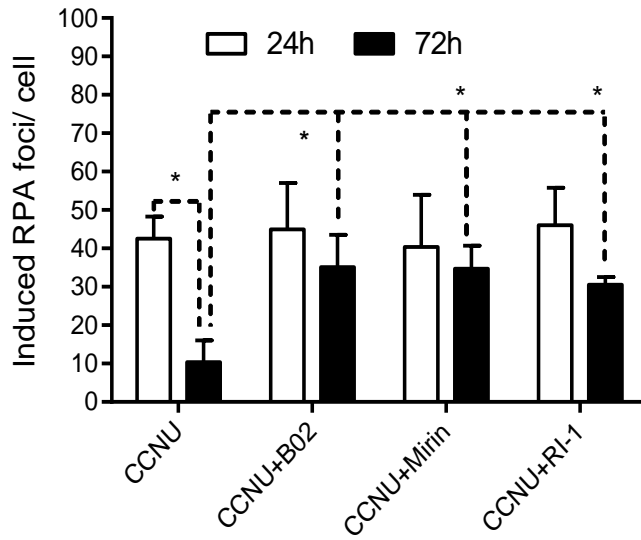


Figure 3

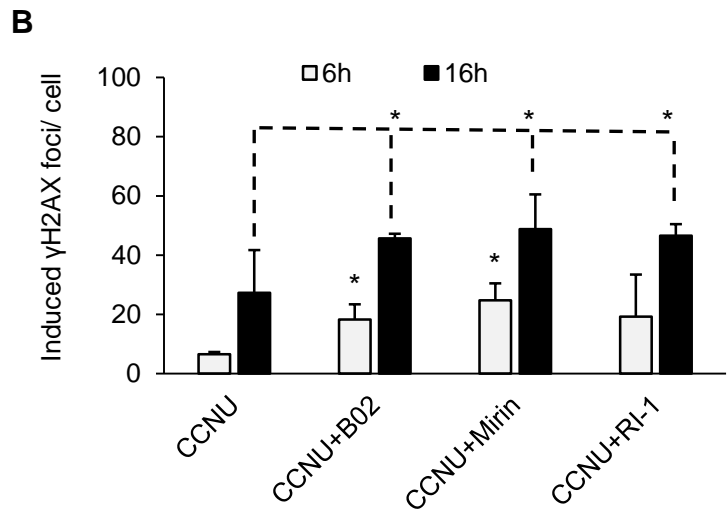
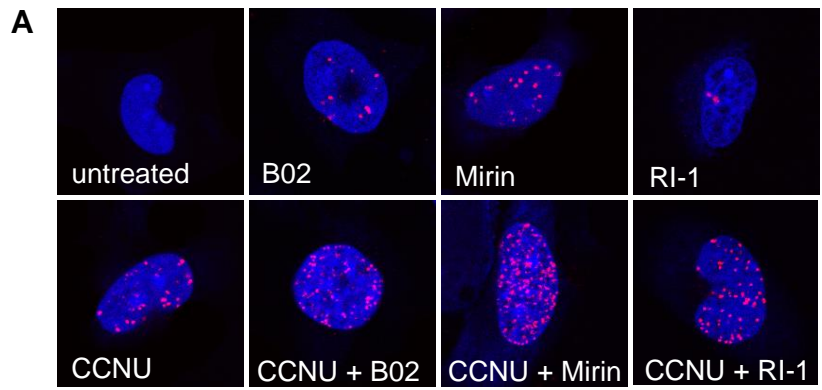


Figure 4

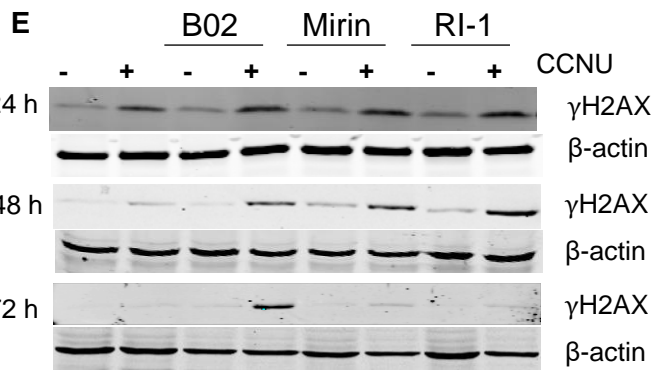
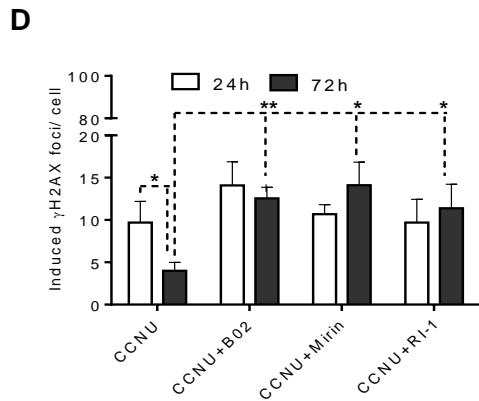
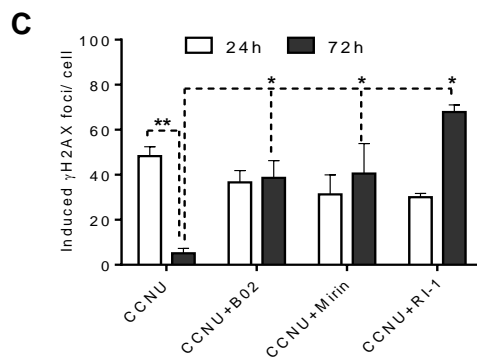
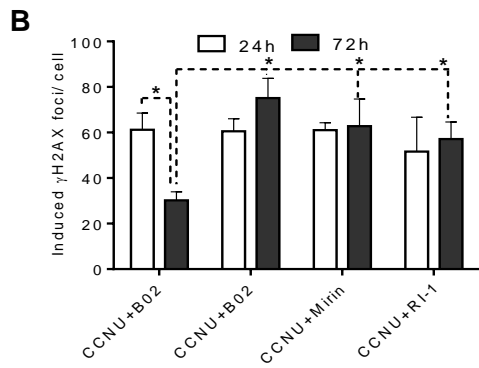
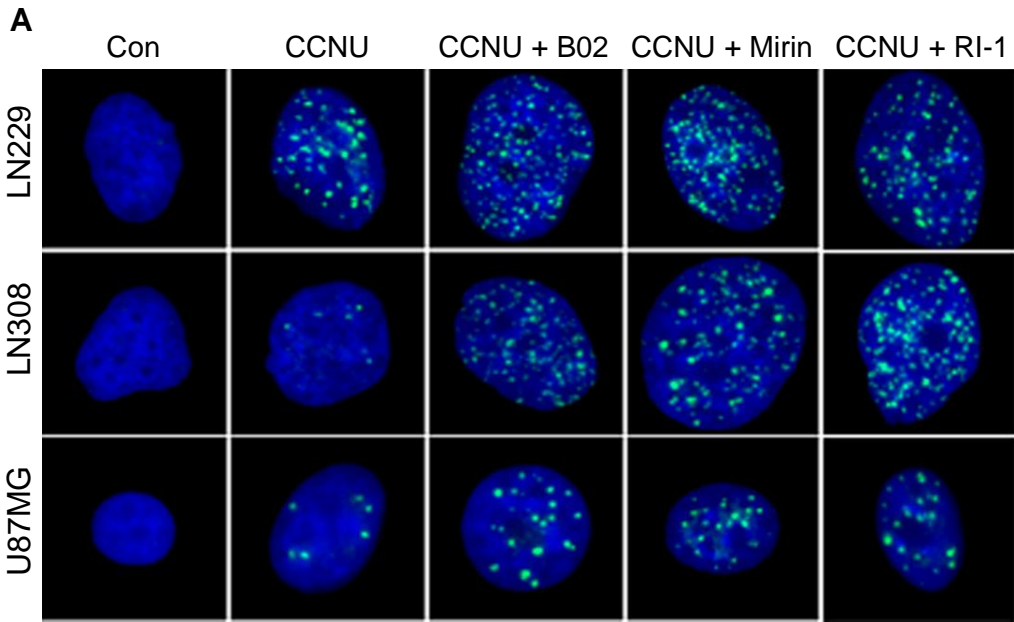


Figure 5

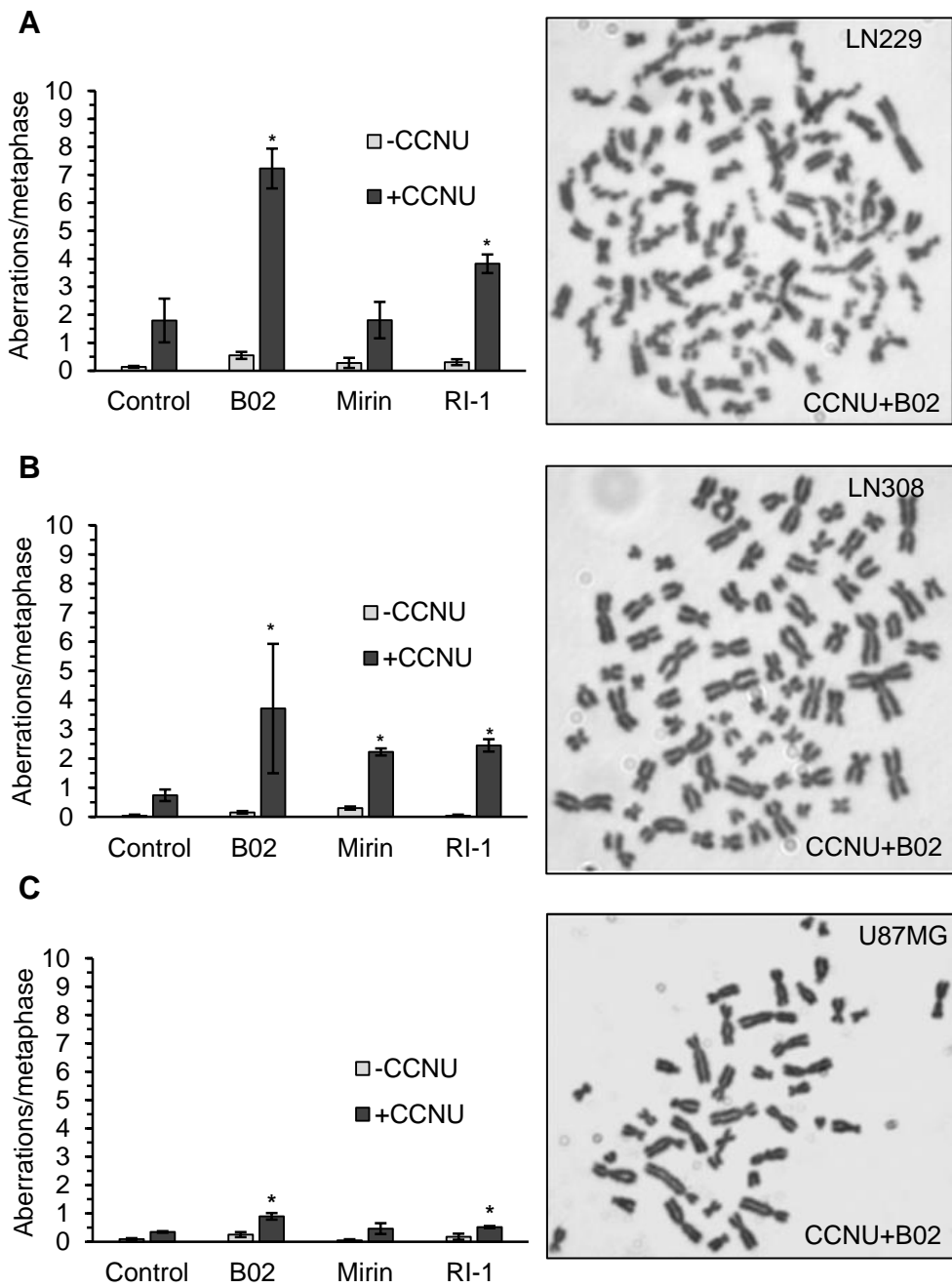


Figure 6

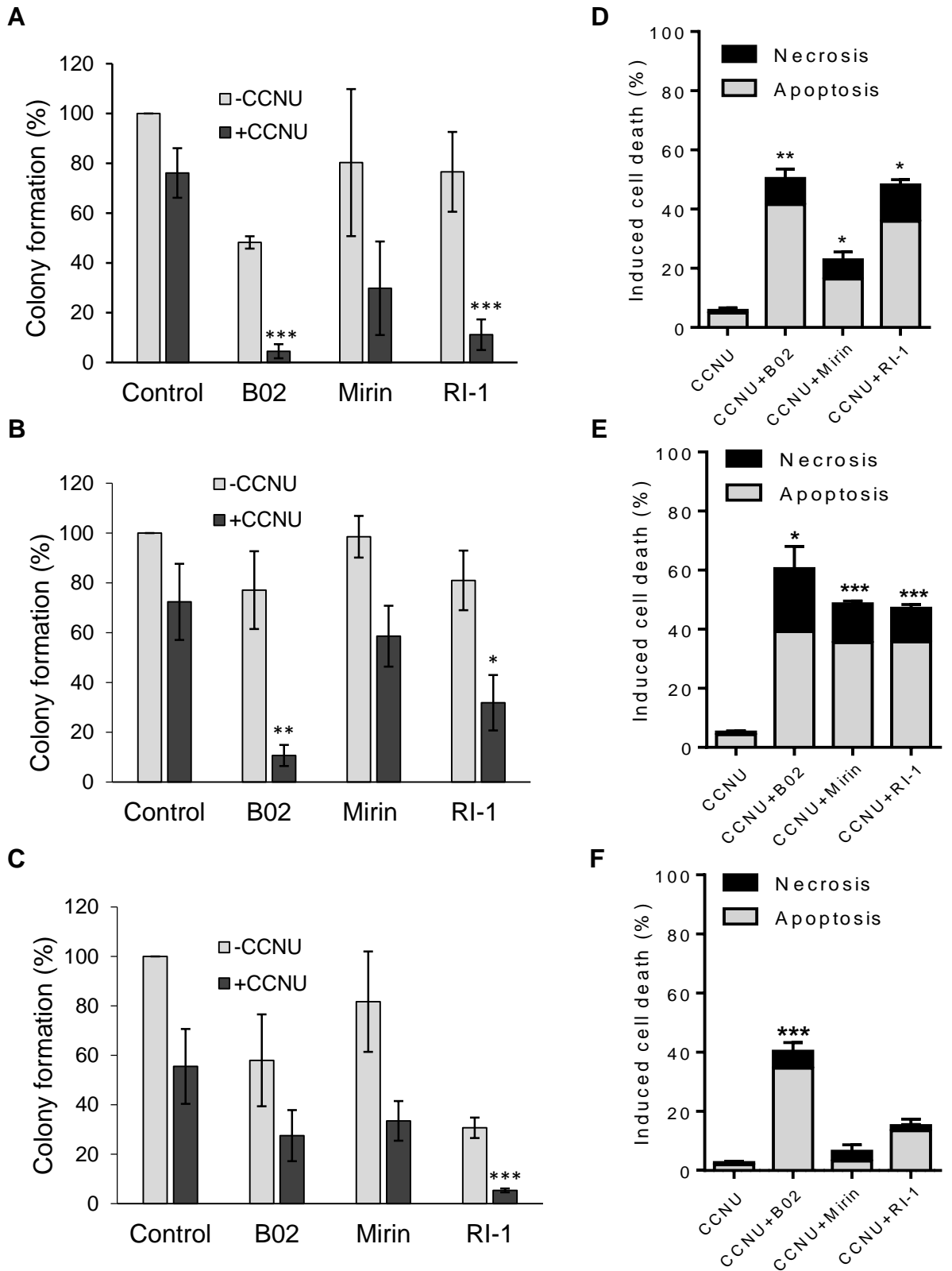


Figure 7

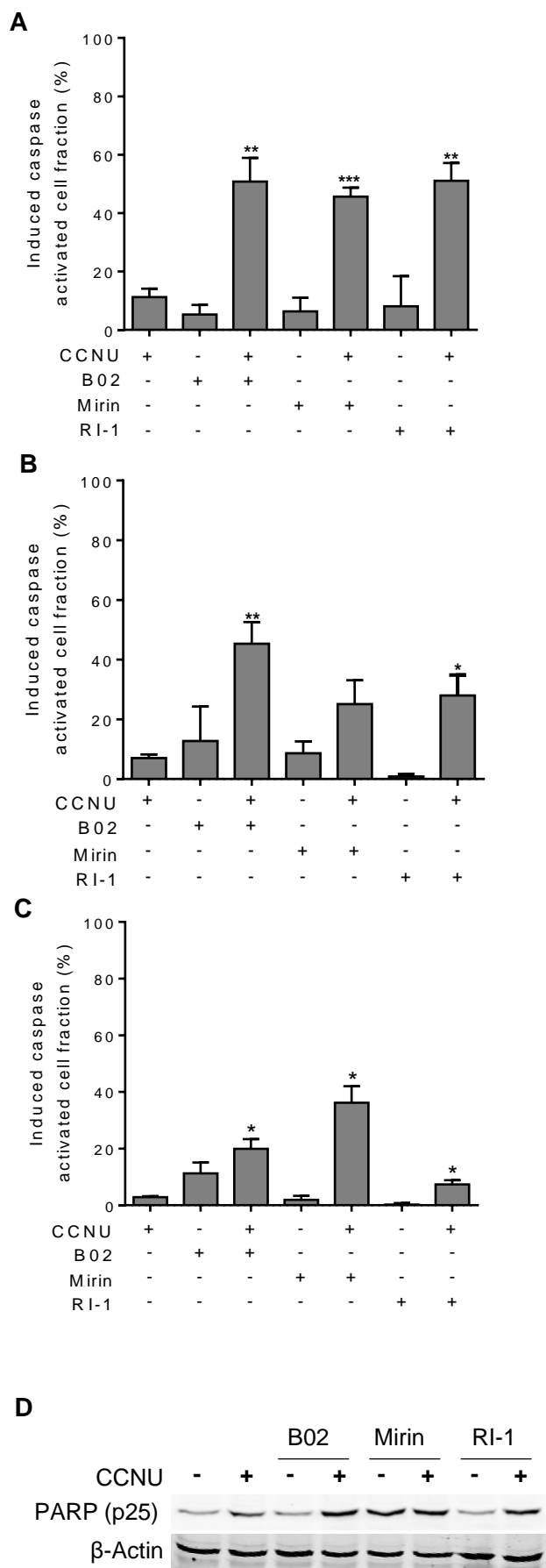


Figure 8

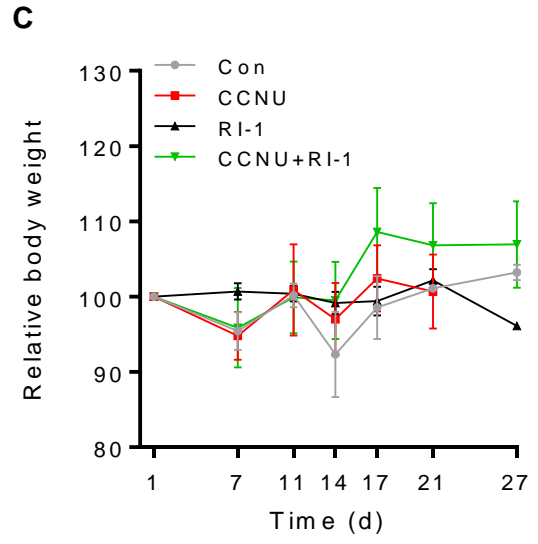
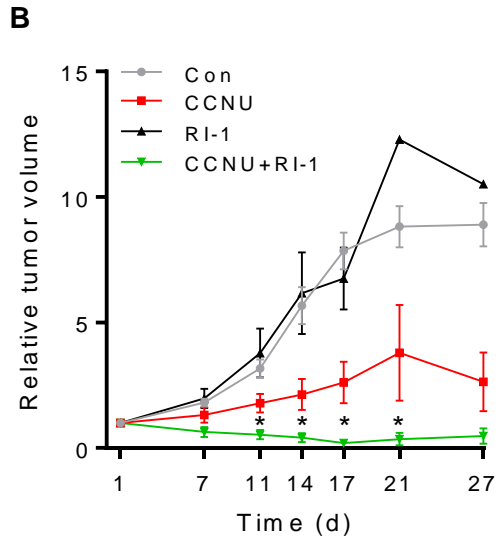
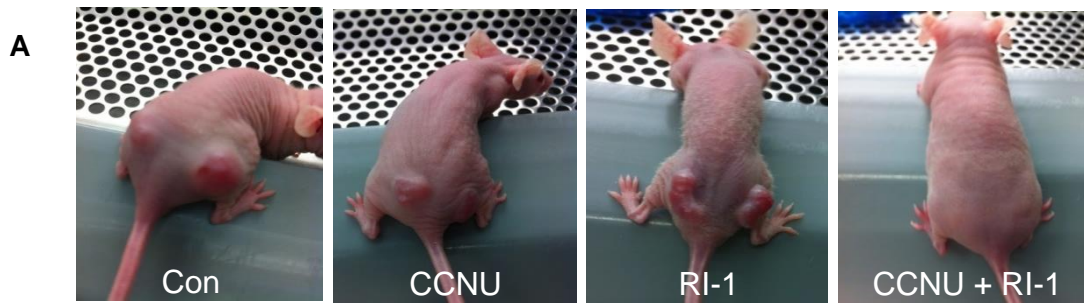


Figure 9